Pergamon

SCIENCE DIRECT

Bioorganic & Medicinal Chemistry 11 (2003) 2751–2759

BIOORGANIC & MEDICINAL CHEMISTRY

Design of Artificial Nucleobases for the Recognition of the AT Inversion by Triple-Helix Forming Oligonucleotides: A Structure–Stability Relationship Study and Neighbour Bases Effect

Dominique Guianvarc'h,[a] Jean-Louis Fourrey,[b] Rosalie Maurisse,[a] Jian-Sheng Sun[a] and Rachid Benhida[b,c,*]

[a]*Laboratoire de Biophysique, UR 565 INSERM, UMR 8646 CNRS, Muséum National d'Histoire Naturelle, 43 rue Cuvier 75231 Paris Cédex 05, France*

[b]*Institut de Chimie des Substances Naturelles, CNRS, 1 avenue de la Terrasse, 91198 Gif-sur-Yvette, France*

[c]*Laboratoire de Chimie Bioorganique, UMR 6001 CNRS, Université de Nice-Sophia Antipolis, Parc Valrose, 06108 Nice Cédex 2, France*

Received 4 February 2003; accepted 1 April 2003

Abstract—We report herein on the synthesis, the incorporation into triplex forming oligonucleotides (TFO) and the recognition properties of a series of synthetic nucleosides designed for the specific recognition of an inverted A•T base pair in a pyrimidine triple helix motif. These analogues were designed on the basis of the results obtained with our previously reported compounds **S** and $\mathbf{B_t}$, in order to define a structure–stability relationship. We report also on the chemical nature effect of the bases flanking **S** in the case of **S**-containing TFOs, in order to get further informations about the recognition process within the A•Tx**S** triplet. This study establishes guidelines for the conception of more potent analogues for the recognition of both A•T and G•C inverted base pairs.

Introduction

Pyrimidine oligonucleotides can interact in a parallel orientation with the oligopurine strand of an oligopyrimidine•oligopurine DNA duplex through the formation of T•AxT and C•GxC$^+$ triplets.[1] This recognition process occurs in the major groove of the double stranded DNA (ds-DNA) and involves the formation of specific Hoogsteen hydrogen bonds between the pyrimidines of the triplex forming oligonucleotide (TFO) and the purine Watson–Crick bases.[2] Accordingly, TFOs have attracted a considerable interest because of their potential applications in gene expression modulation and in gene targeting technologies.[3] Unfortunately, triplex formation by TFOs is limited to oligopyrimidine•oligopurine ds-DNA targets and one observes that a single A•T or G•C base pair interruption reduces strongly the stability of the triplex.[4] To date, the recognition of mixed purine/pyrimidine sequences remains a challenge. In the last few years, two main approaches which involve a number of chemical modifications have been proposed to overcome this sequence limitation.[5] One of these strategies is the universal base approach which consists into conjugating intercalating agents to the 5′- or 3′-end or to internal positions of the TFO in order to stabilise the triplex containing base-pair interruptions in the purine motif.[6] An alternative approach is the specific base strategy which calls for the synthesis of new modified bases able to form hydrogen bonds with one or both partners of the A•T or the G•C Watson–Crick inverted base pairs in the major groove.[7] This specific base approach seems to be a promising way, although in most cases the proposed analogues appear to interact by intercalation rather than by forming specific H-bonds. Moreover, whereas a large number of extended nucleobases have been engineered for the recognition of the G•C base pair,[7] compounds designed for targeting the A•T base pair are still lacking. In this respect, it is noteworthy that the presence of the 5-methyl group of thymine constitutes a supplementary obstacle for the recognition of A•T inversions due to steric hindrance.

We have recently reported on the synthesis and the recognition properties of two non-natural *C*-nucleoside

*Corresponding author. Tel.: +33-492-076153; fax: +33-492-076151; e-mail: benhida@unice.fr

0968-0896/03/$ - see front matter © 2003 Elsevier Science Ltd. All rights reserved.
doi:10.1016/S0968-0896(03)00229-3

analogues **S** and $\mathbf{B_t}$ (see structure in Fig. 1) when incorporated into pyrimidine-motif TFOs.[8] When the thiazolyl-aniline derivative **S** was incorporated into oligonucleotides, the resulting TFO was found to selectively recognise an A•T base pair in ds-DNA with an affinity similar to those obtained in the case of canonical triplets (T•AxT and C•GxC$^+$). On the other hand, we found quite surprisingly the triplex constructed with a TFO containing the thiazolyl-benzimidazole derivative $\mathbf{B_t}$ to be less stable than the analogue incorporating **S**. Indeed, although structurally related to **S**, $\mathbf{B_t}$ is conformationally less flexible than **S** owing to extended aromaticity of the benzimidazole ring. Accordingly, because of favourable entropic factors, we expected $\mathbf{B_t}$ to exhibit more efficient triplex stabilising properties than **S**. In addition, $\mathbf{B_t}$ induced only a moderate discrimination between the A•T and G•C base pairs, suggesting a non sequence-specific interaction with the probe, probably due to base intercalation.

However, the presence of the amino-thiazole moiety in these **S** and $\mathbf{B_t}$ *C*-nucleobases was determinant for their recognition properties. This observation led us to further investigate the recognition process leading to the formation of the A•Tx**S** and A•Tx$\mathbf{B_t}$ triplets. Accordingly, we have designed a series of analogues of the nucleobases **S** and $\mathbf{B_t}$ whose modifications were chosen to delineate the effects of: (i) the nature of the heteroatom X (X = N or S; Fig. 1) facing the 6-amino group of **A** within the A•T base pair, (ii) the length of the linker ($n = 0$ or 1) between the 2-deoxyribose unit and the nucleobase, and (iii) the flexibility/aromaticity of the nucleobase (i.e., aniline with Z = O or benzimidazole with Z = N).

We report here on the synthesis of these analogues, their incorporation into TFOs, together with their recognition properties of an A•T base-pair interruption.

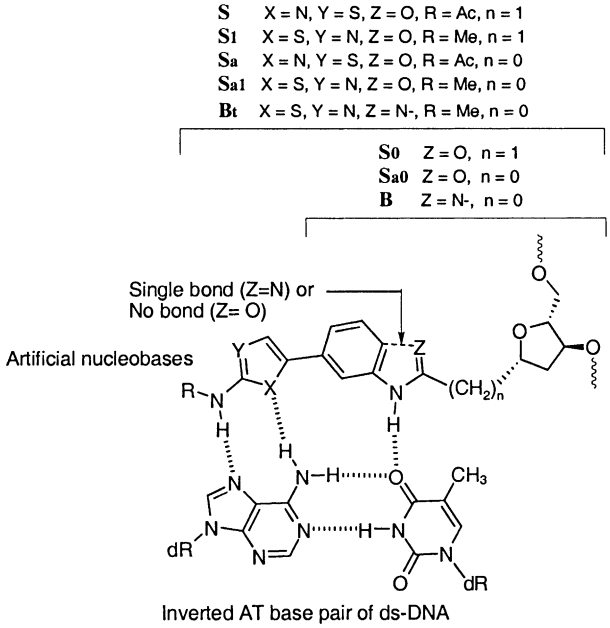

Figure 1. Structure of the artificial nucleobases and proposed model for their specific recognition of an inverted A•T base pair.

In order to have further insight into the recognition process within the A•Tx**S** triplet, we report also on the chemical nature effect of the bases flanking **S** in the case of **S**-containing TFOs.

Results and Discussion

Syntheses

The preparations of the phosphoramidites of **S**, $\mathbf{S_0}$, $\mathbf{B_t}$, and **B** have been described previously.[8] The phosphoramidite derivative of **S1** (i.e., **8**) was obtained by coupling the protected 2-deoxyribose derivative **2** with the 3-iodo-aniline **3** activated as its Weinreb's amide[9] (Scheme 1). Compound **2** was prepared in 85% yield from ester **1** according to literature.[10] The protection of the 3-hydroxyl position being performed with TBDMSCl in DMF. Then, 3-iodo-aniline **3**, activated as its dimethylaluminium derivative, was coupled with **2** to furnish **4** in 90% yield. Compound **6** was prepared using a previously described procedure[11] by application of a palladium catalysed Stille[12] cross-coupling reaction between the 5-(tributyltin)-thiazolyl derivative **5**[13] and the iodo compound **4** in 87% yield. Successive TBDMS cleavage (Bu_4NF, THF) and phosphitylation under standard conditions of the resulting compound **7** provided phosphoramidite **8** in 53% overall yield (two steps).

The synthesis of the carboxamides $\mathbf{S_1}$, $\mathbf{S_a}$, $\mathbf{S_{a0}}$ and $\mathbf{S_{a1}}$ was performed starting from the protected ribonic acid **9** (Scheme 2). Thus, **9** was obtained in two steps from 3,5-di-*O*-toluoyl-α-1-chloro-2-deoxy-D-ribofuranose[14] following nucleophilic substitution (TMSCN) and subsequent hydrolysis of the 1-cyano intermediate (HCl/dioxane).[15] The amide coupling was accomplished in high yield by condensation of **9** with either aniline **10**, compound **11**[8a] or **3** using the Mukaiyama's reagent (2-chloro-1-methylpyridinium iodide).[16] Compound **15** was obtained following Stille-type coupling of the iodo compound **14** with the tin derivative **5**. Selective saponification of the resulting toluoyl esters **12**, **13** and **15** was accomplished using sodium methanolate in methanol, producing **16**, **17** and **18**, respectively, in good yields. Successive 5′-dimethoxytritylation and 3′-phosphitylation of compounds **16**, **17** and **18** under standard conditions provided the corresponding phosporamidites **22**, **23** and **24**, respectively. Phosphoramidites **8**, **22**, **23** and **24** were then incorporated into the 18-mer pyrimidine-motif TFOs (III) listed in Table 1, at the internal position Z using automated oligonucleotide synthesis.

Structure–stability relationship study

The triple helix binding properties of the TFOs III were examined by means of thermal denaturation experiments with the oligopyrimidine•oligopurine 26-mer duplex (I•II) containing an A•T interruption (X•Y = A•T) (Table 1).[17] All the new synthetic thiazolyl $\mathbf{S_1}$, $\mathbf{S_a}$ and $\mathbf{S_{a1}}$ nucleobases, showed a lower capacity to recognise an A•T inverted base pair in ds-DNA than **S**, as shown by the lower T_m values measured for their

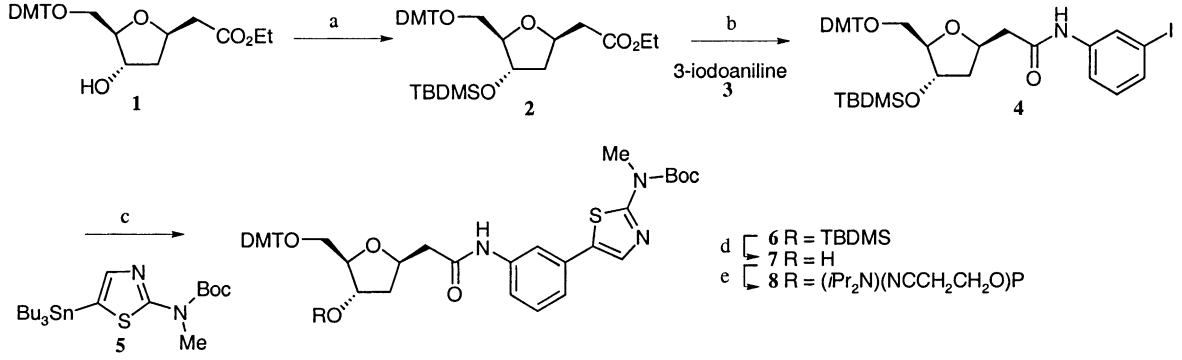

Scheme 1. Synthesis of phosphoramidite **8**. Reagents and reaction conditions: (a) TBDMSCl, imidazole, DMF (85%); (b) $AlMe_3$, molecular sieves 4 Å, toluene, (90%); (c) **5**, $Pd(Ph_3)_4$, DMF, 60 °C (87%); (d) Bu_4NF, THF (87%); (e) $ClP(OCH_2CH_2CN)(NiPr)_2$, *N*,*N*-diisopropylethylamine, CH_2Cl_2 (61%).

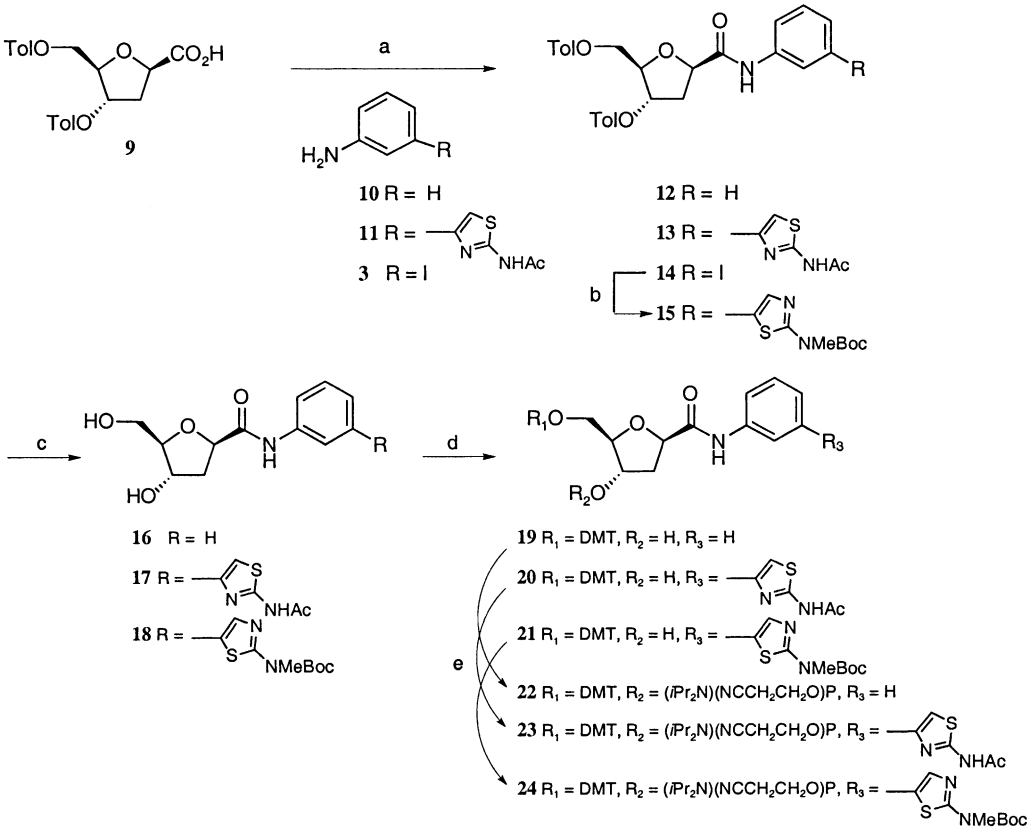

Scheme 2. Synthesis of phosphoramidites **22**, **23** and **24**. Reagents and reaction conditions: (a) chloromethylpyridinium iodide, Et_3N, CH_2Cl_2, 60 °C (90–95%); (b) **5**, $Pd(Ph_3)_4$, DMF, 60 °C (92%); (c) NaOMe, MeOH (91–97%); (d) DMTCl, Et_3N, DMF (80%); (e) $ClP(OCH_2CH_2CN)(NiPr)_2$, *N*,*N*-diisopropylethylamine, CH_2Cl_2 (63–80%).

corresponding triplexes (entries 6, 8 and 9 as compared with entry 5). Interestingly, some observations concerning the structure–stability relationship were obtained from this study and are given below.

Aminothiazole effect. In our preliminary work, we showed that the presence of the aminothiazole moiety of **S** or $\mathbf{B_t}$ was essential since incorporation of $\mathbf{S_0}$ or **B** into the TFO led to an important loss of stability compared with the **S** or **Bt**-based TFOs, respectively ($\Delta T_m = -18$ or -9 °C, respectively).[8] In line with these results, we also found that when going from $\mathbf{S_0}$ to $\mathbf{S_1}$ or from $\mathbf{S_{a0}}$ to $\mathbf{S_a}$ a significant increase of T_m was observed ($\Delta T_m = +12$ or $+7$ °C, respectively). However, the opposite result was obtained when going from $\mathbf{S_{a0}}$ to $\mathbf{S_{a1}}$ ($\Delta T_m = -8$ °C). Moreover, the T_m value of $\mathbf{S_{a1}}$-TFO is identical to the one observed with a truncated 12-mer TFO matching until the Z position as presented in Table 1 ($T_m = 28$ °C, entry 11). Hence, in the triplex with $\mathbf{S_{a1}}$-TFO, the Hoogsteen pairing is likely stopped at the $\mathbf{S_{a1}}$ site, and all the $\mathbf{S_{a1}}$TTCTT bases are not associated. Furthermore, the *T*m value obtained with $\mathbf{S_{a0}}$-TFO ($T_m = 36$ °C, entry 10) suggests that the Hoogsteen pairing of the five 3′-end bases of this TFO is partially destroyed.

Thiazole *endo*-heteroatom effect. The effect of the heteroatom nature (X = N or S; Fig. 1) facing the 6-amino group of **A** within the A•T base pair is shown by com-

Table 1. Sequence of the I•IIxIII triplexes and melting temperature values (T_m ±1 °C)

3′-CGTA-TTTTCTTCTCTT**X**TTCTT-AGTG-5′	I
5′-GCAT-AAAAGAAGAGAA**Y**AAGAA-TCAC-3′	II
5′-TTTTCTTCTCTT**Z**TTCTT-3′	III
5′-TTTTCTTCTCTT-3′	Truncated TFO

Entry	X•Y (ds-DNA I•II)	Z (TFO III)	Structure of the nucleobase	T_m (°C)
1	T•A	**T**	—	51
2	A•T	**G**	—	45
3	A•T	$\mathbf{B_t}$	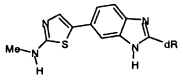	43
4	A•T	**B**		34
5	A•T	**S**	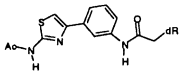	50
6	A•T	$\mathbf{S_1}$	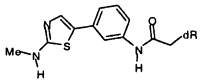	44
7	A•T	$\mathbf{S_0}$	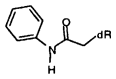	32
8	A•T	$\mathbf{S_a}$	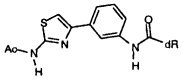	43
9	A•T	$\mathbf{S_{a1}}$	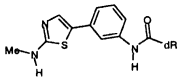	28
10	A•T	$\mathbf{S_{a0}}$	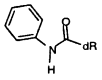	36
11	I•II	A truncated 12 mer TFO		28

parison of $\mathbf{S}/\mathbf{S_1}$ and $\mathbf{S_a}/\mathbf{S_{a1}}$ (Table 1). Thus, **S** and $\mathbf{S_a}$ differ from $\mathbf{S_1}$ and $\mathbf{S_{a1}}$ respectively by the position of attachment of the aminothiazole moiety to the phenyl ring, the thiazole being linked at C-5 in $\mathbf{S_1}$ and $\mathbf{S_{a1}}$ whereas it is connected at C-4 in the case of **S** and $\mathbf{S_a}$. Both nucleobases possess the required amino group (NH) for the recognition of the adenine N7 nitrogen. We found that the stabilisation increased when going from **S1** to **S** ($\Delta T_m = +6$ °C) or from $\mathbf{S_a}$ to $\mathbf{S_{a1}}$ ($\Delta T_m = +15$ °C). This result indicates that the best triplex stabilisation could be obtained with aminothiazole in which the nitrogen *endo* is involved in the recognition of the adenine (NH_2) Watson–Crick base rather than sulfur.

Linker effect. Incorporation of $\mathbf{S_a}$ into the TFO led to a less stable triplex compared to the one containing **S** ($\Delta T_m = -7$ °C). This compound only differs by the length of the linker between the sugar unit and the aglycone part, **S** featuring a supplementary methylene. Accordingly, the length of the linker in the case of **S** seems to be well adapted for the recognition of the A•T inverted base pair. Comparison of the T_m values of $\mathbf{S_1}$ (entry 6, $T_m = 44$ °C) and $\mathbf{S_{a1}}$ (entry 9, $T_m = 28$ °C) leads to a similar observation, the decrease being $\Delta T_m = -16$ °C.

Flexibility/aromaticity of nucleobase. One can observe that $\mathbf{B_t}$ possesses the same ability to form hydrogen bond contacts as $\mathbf{S_{a1}}$. However, the $\mathbf{S_{a1}}$-TFO forms a less stable triplex with ds-DNA than the $\mathbf{B_t}$-TFO (entries 3 and 9, $\Delta T_m = -15$ °C). This low stability obtained with $\mathbf{S_{a1}}$-TFO corresponds to the one observed in the case of the truncated triplex (entry 11, $T_m = 28$ °C). As there is a great structural analogy between the aglycone part of the two heterocyclic systems of $\mathbf{B_t}$ and $\mathbf{S_{a1}}$, this result should be likely ascribed to conformational factors. Indeed, in the case of compound $\mathbf{S_{a1}}$, the ring oxygen of deoxyribose and of the carbonyl amide function can adopt a *trans* or *cis* relationship by rotation around the glycosidic C1′–CO bond (Fig. 2).

The *cis* conformation is expected to be defavourable because of the oxygen–oxygen anomeric effect. Unfortunately, the thermodynamically stable *trans* conformation induced a base orientation change which destroyed the base pairing at the interrupted site, resulting in a triplex destabilisation. In the case of **Bt**, the highly delocalised electronic charge on the benzimidazole ring and the hydrogen prototropy disfavoured the anomeric effect and hence, favoured the free rotation around the C–C glycosidic bond. In this case, both conformations could exist without any energetic penalty. In contrast, in the case of $\mathbf{S_a}$-TFO, the moderate *T*m value ($T_m = 43$ °C, entry 8) might reflect favourable interactions with the A•T base pair preventing this moiety to adopt a *trans* conformation. Indeed, the best aminothiazole system of $\mathbf{S_a}$ could compensate the anomeric effect keeping the nucleobase in the best conformation for adenine recognition.

Nearest-neighbour effects around the A•TxS non-natural base triplet

In order to get further informations about the stabilising effect observed within the triple helice containing the A•Tx**S** triplet (Table 1, entry 5), we investigated the effect of the base triplets flanking the A•Tx**S** one on the triplex stabilisation process (X_1•Y_1xZ_1 and X_2•Y_2xZ_2 triplets). Towards this end, **S** and **G** (as a control) were incorporated into the 18-mer TFO (III) at the internal position Z flanked by C^+ and/or T at positions Z_1 and Z_2. The triple helix binding properties of these TFOs harbouring the four possible combinations (Table 2, entries 1 to 4, $Z_1\mathbf{Z}Z_2 = \mathbf{TST}$, $\mathbf{TSC^+}$, $\mathbf{C^+ST}$, $\mathbf{C^+SC^+}$) were examined by means of thermal denaturation experiments with their respective 26-mer ds-DNA (I•II) target.

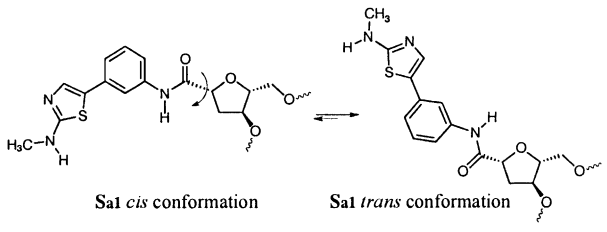

Figure 2. *trans* and *cis* conformations of compound $\mathbf{S_{a1}}$.

Table 2. Nearest-neighbour effects within triplexes containing **S** (or **G**) in the Hoogsteen-paired strand (III)

3′-CGTA-TTTTCTTCTCT**X_1AX_2**TCTT-AGTG-5′ I
5′-GCAT-AAAAGAAGAGA**Y_1TY_2**AGAA-TCAC-3′ II
5′-TTTTCTTCTCT**Z_1ZZ_2**TCTT-3′ III

Entry	Triplet X_1•Y_1xZ_1	Triplet X_2•Y_2xZ_2	T_m (°C)	
			Z = **G**	Z = **S**
1	T•AxT	T•AxT	45	50
2	T•AxT	C•GxC$^+$	41	43
3	C•GxC$^+$	T•AxT	41	43
4	C•GxC$^+$	C•GxC$^+$	34	40

As shown in Table 2, a neighbour bases effect was observed with the non-natural A•Tx**S** triplet. Indeed, the triple helix was most stable when A•Tx**S** triplet was flanked by two T•AxT triplets. In contrast, the stability of the triplexes decreased as the number of adjacent C•GxC$^+$ around A•Tx**S** triplet increased. Although, we did not find any 5′- or 3′-C•GxC$^+$ side effect (entries 2 and 3, $T_m = 43$ °C). Finally, in all cases, the A•Tx**S** triplet provides a better triplex stabilisation compared to the best natural base triplet A•Tx**G**. This stabilisation is moderate ($\Delta T_m = +2$ °C) when the A•Tx**S** triplet is flanked by T•AxT and C•GxC$^+$ neighbours in either the 5′- or the 3′-direction (entries 2 and 3, respectively). In contrast, this stabilisation is higher when the A•Tx**S** triplet is flanked by two T•AxT, ($\Delta T_m = +5$ °C) or two C•GxC$^+$ triplets ($\Delta T_m = +6$ °C).

Previously, Dervan et al. have examined the effects of altering the flanking sequence around an A•Tx**G** triplet using the affinity cleaving method.[18,19] Both results are in accordance excepting that, in our case, we did not observe any 3′- or 5′-C•GxC$^+$ side effects (entries 2 and 3, $T_m = 41$ °C).

Altogether, these results indicate that the use of compound **S** for the recognition of an inverted A•T base pair is more favourable than **G** whatever the sequence composition. In contrast to the reported work,[20] the neighbour bases effect, in our case, is the same on both the 3′- and 5′-sides. This might suggest that the mode of interaction of **S** probably depends more on favourable hydrogen bond contacts rather than on base intercalation. Although, the base stacking contributions will play an important role in the overall triplex stabilisation.

Conclusion

In summary, we synthesised a series of nucleoside analogues featuring highly functionalised nucleobases. To the best of our knowledge, **S** is the best nucleobase analogues for the recognition of an A•T base pair inversion since it gives a high increase of triplex stability. Moreover, the structure–stability relationship study of these compounds establishes guidelines for the design of more potent analogues for the recognition of both A•T and C•G inverted base pairs. Indeed, in the continuation of this project, the synthesis of new cyclised analogues related to the benzimidazole series is in progress, in order to increase the triplex stability and natural base pairs discrimination. Furthermore, the neighbour effect of the base pairs flanking the A•T inversion provides some informations about the interactions stabilising the non-natural A•Tx**S** triplet. Thus, it was found that in all cases, the triplexes containing the A•Tx**S** triplet are more stable than those containing the A•Tx**G** one. This gain of stability is more important for the triplexes in which **S** is flanked on each side by T or C$^+$. Finally, it was found that neighbour base effect, i.e., destabilisation in presence of C$^+$, is the same on the 5′-side as on the 3′-side favouring the proposed selective hydrogen bonds binding mode.

Experimental

General

Solvents were dried by standard methods. All reagents were of commercial quality (Acros, Aldrich or Lancaster) and were used without further purification. Melting points were determined with a Kofler apparatus and are uncorrected. Microanalyses were performed by the 'Service de Microanalyses de l'ICSN-CNRS'. ^{1}H, ^{13}C and ^{31}P NMR spectra were conducted on Bruker AC250, AM300 and AM400 spectrometers. NMR chemical shifts (δ) are given in ppm relative to TMS (^{1}H) or H_3PO_4 (^{31}P). Mass spectra were recorded on a AEI MS-9 (CI), KRATOS MS-80-RF (FAB). Column chromatography were carried out on Silica gel Merck Kiesegel 60 (230–400 mesh). Analytic TLC were performed using Merck silica gel 60 F_{254}, the spots were visualized with UV/vis light, iodine or phosphomolybdic acid spray followed by heating. HPLC analyses were recorded on Gilson apparatus. All reactions were carried out under a nitrogen atmosphere under anydrous conditions unless otherwise noted.

Ethyl-(2-deoxy-3-*O*-*tert*-butyldimethylsilyl-5-*O*-dimethoxytrityl-β-D-ribofuranosyl)-acetate (2). To a solution of compound **1** (216 mg, 0.42 mmol) in DMF (5 mL) were successively added imidazole (6 equiv, 163 mg) and TBDMSCl (3.2 equiv, 181 mg). The reaction mixture was stirred for 16 h at room temperature, then evaporated under reduced pressure to give a crude oil. Silica gel column chromatography purification using a gradient of ethyl acetate in heptane with triethylamine (1%) afforded **2** as an oil (221 mg, 85%). R_f 0.65 (7:3 heptane/ethyl acetate). ^{1}H NMR ($CDCl_3$) δ 0.02 (2s, 6H), 0.83 (s, 9H), 1.21 (t, 3H, $J = 7.1$ Hz) 1.70 (m, 1H), 1.95 (m, 1H), 2.50 (m, 2H), 2.65 (m, 2H), 3.06 (m, 2H), 3.73 (s, 6H), 3.91 (m, 1H), 4.13 (q, 2H, $J = 7.1$ Hz), 4.25 (m, 1H), 4.50 (m, 1H), 6.80 and 7.30 (m, 8H), 7.10–7.50 (m, 5H). ^{13}C NMR ($CDCl_3$) δ 14.21, 17.98, 25.78, 40.77, 41.09, 55.12, 60.41, 64.14, 74.25, 74.62, 85.98, 86.58, 113.04, 126.67, 127.72, 128.21, 130.08, 136.18, 145.0, 158.42, 171.10. MS (FAB) $m/z = 643$ $[M + Na]^+$.

***C*-(3′-*O*-(*tert*-Butyldimethylsilyl)-2′-deoxy-5′-*O*-dimethoxytrityl-β-D-ribofuranosyl-1′)-*N*-(3-iodophenyl) carboxamide (4).** To a solution of 2-iodo-aniline **3** (3 equiv, 212 mg) in dry toluene (5 mL) in the presence of molecular sieves (4 Å), was added dropwise at 0 °C a 2 M $AlMe_3$ solution in toluene (3 equiv, 0.5 mL) under argon atmosphere. After stirring for 2 h at room temperature, a solution of compound **2** (200 mg, 0.32 mmol) in toluene was added and the reaction mixture was stirred for 2 h at room temperature. Then, the reaction mixture was poured into aq $NaHCO_3$ solution and extracted with ethyl acetate. The organic layer was dried over $MgSO_4$, filtred and the solvent removed in vacuo. The crude residue was purified by silica gel chromatography using methylene chloride/ethyl acetate as solvents with triethylamine (1%) to provide **4** as an oil (230 mg, 90%). R_f 0.50 (7:3 heptane/ethyl acetate). ^{1}H NMR ($CDCl_3$) δ 0.02 (2s, 6H), 0.85 (s, 9H), 1.75 (m, 1H), 1.95 (m, 1H), 2.49 (m, 2H), 2.62 (dd, 2H, J = 3.0 and 15.0 Hz), 3.2 (m, 2H), 3.75 (s, 6H), 4.05 (m, 1H), 4.25 (m, 1H), 4.55 (m, 1H), 6.80 (m, 4H), 6.9 (t, 1H, J = 8.1 Hz), 7.10–7.45 (m, 11H), 7.85 (s, 1H), 8.55 (s, 1H). ^{13}C NMR ($CDCl_3$) δ 4.54, 18.03, 25.86, 41.24, 43.58, 55.29, 64.07, 73.78, 74.94, 86.32, 87.24, 94.18, 113.23, 119.06, 127.93, 128.23, 128.42, 129.25, 130.10, 130.39, 132.97, 135.91, 139.40, 144.82, 158.60, 169.29. MS (FAB) m/z = 816 $[M+Na]^+$.

***C*-(3′-*O*-(*tert*-Butyldimethylsilyl)-2′-deoxy-5′-*O*-dimethoxytrityl-β-D-ribofuranosyl-1′)-*N*-[3-(2-*N*-methyl-*N*-*tert*-butoxycarbonyl-thiazole-5-yl)phenyl]acetamide (6).** To a solution of compound **4** (660 mg, 0.83 mmol) in dry DMF (10 mL) were successively added, under argon atmosphere, thiazolyltin derivative **5** (1.5 equiv, 800 mg) and $Pd(PPh_3)_4$ (80 mg). The mixture was stirred at 60 °C for 2 h and then filtred through Celite. The filtrate was evaporated to give a crude residue which was purified by flash chromatography on silica gel, using 20% of ethyl acetate in heptane with triethylamine (1%), to afford **6** as an oil (635 mg, 87%). R_f 0.30 (7:3 heptane/ethyl acetate). ^{1}H NMR ($CDCl_3$) δ 0.02 (2s, 6H), 0.85 (s, 9H), 1.59 (s, 9H), 1.75 (m, 1H), 1.95 (m, 1H), 2.59 (m, 1H), 2.70 (m, 1H), 3.20 (m, 2H), 3.56 (s, 3H), 3.75 (s, 6H), 4.05 (m, 1H), 4.25 (m, 1H), 4.56 (m, 1H), 6.80 and 7.30 (m, 8H), 7.10 and 7.40 (m, 7H), 7.43 (m, 1H), 7.55 (s, 1H), 7.70 (s, 1H), 8.52 (s, 1H). ^{13}C NMR ($CDCl_3$) δ −4.62, 18.90, 25.79, 28.27, 33.94, 41.30, 43.69, 55.17, 64.01, 73.79, 74.95, 86.24, 87.25, 113.14, 117.18, 118.97, 121.8, 126.86, 127.84, 128.17, 129.48, 130.01, 132.90, 133.01, 133.40, 135.87, 138.73, 145.10, 153.50, 158.51, 162.30, 169.28. MS (FAB) m/z = 902 $[M+Na]^+$.

***C*-(2′-Deoxy-5′-*O*-dimethoxytrityl-β-D-ribofuranosyl-1′)-*N*-[3-(2-*N*-methyl-*N*-*tert*-butoxycarbonyl-thiazole-5-yl)-phenyl]acetamide (7).** Compound **6**(457 mg, 0.52 mmol) was dissolved in THF (15 mL) and 1 M TBAF in THF (1.1 equiv, 0.6 mL) was added. The reaction mixture was stirred at room temperature for 1 h and then evaporated to a syrup. The residue was purified over a silica gel column, using 20% of ethyl acetate in heptane, to afford **7** as a white foam (345 mg, 87%). ^{1}H NMR ($CDCl_3$) δ 1.59 (s, 9H), 1.90 (m, 1H), 2.08 (m, 1H), 2.59 (m, 1H), 2.67 (m, 1H), 3.25 (m, 2H), 3.56 (s, 3H), 3.73 (s, 6H), 4.07 (m, 1H), 4.37 (m, 1H), 4.57 (m, 1H), 6.80 and 7.30 (m, 8H, H–Ar), 7.10–7.40 (m, 7H), 7.43 (m, 1H), 7.56 (s, 1H), 7.68 (s, 1H), 8.43 (s, 1H). ^{13}C NMR ($CDCl_3$) δ 28.21, 33.94, 40.98, 43.57, 55.12, 64.35, 73.51, 74.91, 86.23, 86.67, 113.13, 117.21, 119.04, 121.83, 126.85, 127.83, 128.10, 129.47, 129.98, 130.02, 132.94, 133.29, 135.81, 138.60, 144.71, 153.10, 158.46, 160.88, 169.30. MS (FAB) m/z = 788 $[M+Na]^+$, 303 $[DMT]^+$.

Phosphoramidite (8). A solution of compound **7** (200 mg, 0.26 mmol) and *N,N*′-diisopropylethylamine (96 μL, 2 equiv) in 5 mL of anhydrous methylene chloride, under an inert atmosphere, was treated with 2-cyanoethyl diisopropylchlorophosphoramidite (68 μL, 1.2 equiv). After stirring for 15 min at room temperature, the reaction mixture was poured into aq $NaHCO_3$ solution, extracted and whashed twice with water. The organic layer was separated, dried over $MgSO_4$, filtred and the solvent removed in vacuo. The crude residue was purified by silica gel chromatography using heptane/ethyl acetate (9/1) as solvents with triethylamine (1%) to provide **8** as a white foam (155 mg, 61%, mixture of two diastereoisomers). R_f 0.44 and 0.51 (1:1 heptane/ethyl acetate). ^{31}P NMR ($CDCl_3$, 243 MHz) δ 145.02, 145.19.

***C*-(2′-Deoxy-3′,5′-di-*O*-toluoyl-β-D-ribofuranosyl-1′)-*N*-phenylcarboxamide (12).** The compound **9** (600 mg, 1.5 mmol) was dissolved in dry methylene chloride (30 mL) and then triethylamine (2 equiv, 4.18 mL), chloromethyl pyridinium iodide (2 equiv, 766 mg) and aniline chlorhydrate **10** (1 equiv, 195 mg) were added successively. After refluxing for 1 h, the solvent was evaporated and the crude product was extracted with methylene chloride, dried over $MgSO_4$, filtred and evaporated. The obtained oil was purified under silica gel chromatography using heptane/ethyl acetate (9/1) as solvants giving 675 mg (95%) of **12** as a white solid. R_f 0.38 (7:3 heptane/ethyl acetate). Mp 123–125 °C. ^{1}H NMR ($CDCl_3$) δ 2.34 (s, 3H), 2.37 (m, 1H), 2.41 (s, 3H), 2.71 (dd, 1H, J = 14.0 and 6.1 Hz), 4.56 (m, 1H), 4.67 (dd, 1H, J = 4.6 and 11.9 Hz), 4.82 (m, 2H), 5.53 (d, 1H, J = 4.8 Hz), 7.01 (m, 2H), 7.26 (m, 5H), 7.61 (d, 2H, J = 8.1 Hz), 7.87 (dd, 2H, J = 1.3 and 8.1 Hz), 7.96 (dd, 2H, J = 1.3 and 8.1 Hz), 8.65 (s, 1H). ^{13}C NMR ($CDCl_3$) δ 21.67, 21.74, 37.25, 64.17, 76.05, 79.14, 84.99, 119.83, 124.40, 126.53, 128.86, 129.30, 129.74, 129.78, 137.34, 144.34, 144.45, 166.16, 166.87, 169.28. MS (IC) m/z = 474 $[M+H]^+$, 353 $[M\text{-}PhNHCO+H]^+$, 119 $[Tol]^+$. Anal. calcd for $C_{28}H_{27}NO_6$: C, 71.02; H, 5.75; N, 2.96. Found: C, 70.79; H, 5.81; N, 2.72.

***C*-(2′-Deoxy-3′,5′-di-*O*-toluoyl-β-D-ribofuranosyl-1′)-*N*-[3-(2-acetylaminothiazole-4-yl)phenyl]carboxamide (13).** By the same procedure as described for the synthesis of **12**, the acid **9** (400 mg, 1 mmol) and the amine **11** (1.5 equiv, 300 mg) were coupled to give compound **13** (white solid, 582 mg, 95%). R_f 0.44 (1:1 heptane/ethyl acetate). Mp 204–206 °C. ^{1}H NMR ($CDCl_3$) δ 2.13 (s, 3H), 2.28 (s, 3H), 2.36 (m, 1H), 2.42 (s, 3H), 2.70 (dd, 1H, J = 6.2 and 13.9 Hz), 4.57 (m, 1H), 4.67 (dd, 1H, J = 12.0 and 4.9 Hz), 4.81 (m, 2H), 5.52 (d, 1H, J = 7.6

Hz), 7.05 (s, 1H), 7.08 (d, 1H, $J=8.1$ Hz), 7.28 (m, 4H), 7.51 (d, 1H, $J=8.1$ Hz), 7.60 (d, 1H, $J=8.1$ Hz), 7.84 (d, 2H, $J=8.2$ Hz), 7.93 (d, 2H, $J=8.2$ Hz), 8.01 (m, 1H), 8.78 (s, 1H). ^{13}C NMR ($CDCl_3$) δ 21.71, 21.82, 23.15, 37.33, 64.28, 76.07, 79.25, 85.11, 108.18, 117.69, 119.56, 122.28, 128.98, 129.38, 129.79, 129.87, 130.17, 137.88, 149.17, 167.02, 169.56. MS (ES) $m/z=614$ $[M+H]^+$. Anal. calcd for $C_{33}H_{31}N_3O_7S$: C, 64.59; H, 5.09; N, 6.85. Found: C, 64.28; H, 5.03; N, 6.49.

***C*-(2′-Deoxy-3′,5′-di-*O*-toluoyl-β-D-ribofuranosyl-1′)-*N*-(3-iodophenyl)carboxamide (14).** By the same procedure as described for the synthesis of **12**, the acid **9** (500 mg, 1.25 mmol) and the 2-iodo-aniline **3** (1.1 equiv, 300 mg) were coupled to give compound **14** (white foam, 674 mg, 90%). R_f 0.5 (7:3 heptane/ethyl acetate). ^{1}H NMR ($CDCl_3$) δ 2.30 (m, 1H), 2.38 (s, 3H), 2.43 (s, 3H), 2.74 (m, 1H), 4.56 (m, 1H), 4.64 (dd, 1H, $J=11.7$ and 4.8 Hz), 4.76 (dd, 1H, $J=6.1$ and 10.6 Hz), 4.85 (dd, 1H, $J=2.1$ and 11.7 Hz), 5.53 (d, 1H, $J=5.7$ Hz), 7.00 (t, 1H, $J=7.9$ Hz), 7.16 (d, 2H, $J=8.0$ Hz), 7.28 (d, 4H, $J=7.7$ Hz), 7.42 (d, 1H, $J=7.8$ Hz), 7.64 (dd, 1H, $J=1.3$ and 8.1 Hz), 7.86 (d, 2H, $J=8.3$ Hz), 7.99 (d, 2H, $J=8.3$ Hz), 8.00 (d, 1H, $J=1.7$ Hz), 8.65 (s, 1H). ^{13}C NMR ($CDCl_3$) δ 21.88, 37.35, 64.19, 76.08, 79.22, 85.26, 90.94, 119.07, 126.41, 128.59, 129.42, 129.49, 129.85, 130.41, 133.45, 138.60, 144.63, 166.28, 167.16, 169.45. MS (IC) $m/z=600$ $[M+H]^+$, 474 $[M-I+H]^+$, 119 $[Tol]^+$. Anal. calcd for $C_{28}H_{26}INO_6$: C, 56.11; H, 4.37; N, 2.34. Found: C, 56.29; H, 4.44; N, 2.45.

***C*-(2′-Deoxy-3′,5′-di-*O*-toluoyl-β-D-ribofuranosyl-1′)-*N*-[3-(2-*N*-methyl-*N*-*tert*-butoxycarbonyl-thiazole-5-yl) phenyl]carboxamide (15).** To a solution of compound **14** (530 mg, 0.88 mmol) in dry DMF (10 mL) were successively added, under Argon atmosphere, thiazolyltin derivative **5** (1.2 equiv, 542 mg), $Pd(PPh_3)_4$ (60 mg) and CuI (10 mg). The mixture was stirred at 65 °C for 1 h and then filtred through Celite. The filtrate was evaporated to give a crude residue which was purified by flash chromatography on silica gel, using 20% of ethyl acetate in heptane, to afford **15** as a white foam (555 mg, 92%). R_f 0.69 (1:1 heptane/ethyl acetate). ^{1}H NMR ($CDCl_3$) δ 1.60 (s, 9H), 2.32 (s, 3H), 2.35 (m, 1H), 2.43 (s, 3H), 2.75 (m, 1H), 3.57 (s, 3H), 4.57 (m, 1H), 4.70 (dd, 1H, $J=12.0$ and 4.9 Hz), 4.82 (m, 2H), 5.54 (d, 1H, $J=5.7$ Hz), 7.12 (d, 2H, $J=7.9$ Hz), 7.27 (m, 4H), 7.58 (m, 2H), 7.77 (s, 1H), 7.87 (d, 2H, $J=8.2$ Hz), 7.93 (d, 2H, $J=8.2$ Hz), 8.71 (s, 1H). ^{13}C NMR ($CDCl_3$) δ 21.73, 21.83, 28.34, 34.04, 37.35, 64.26, 76.11, 79.29, 85.22, 117.30, 118.95, 122.22, 126.53, 129.41, 129.55, 129.85, 132.87, 133.08, 133.47, 138.04, 144.54, 166.0, 167.03, 169.51. MS (FAB) $m/z=708$ $[M+Na]^+$, 119 $[Tol]^+$. Anal. calcd for $C_{37}H_{39}N_3O_8S$: C, 64.80; H, 5.73; N, 6.13. Found: C, 64.56; H, 5.74; N, 5.96.

***C*-(2′-Deoxy-β-D-ribofuranosyl-1′)-*N*-phenylcarboxamide (16).** To a stirred solution of compound **12** (300 mg, 0.634 mmol) in dry MeOH (10 mL) was added MeONa (3 equiv, 102 mg). The reaction mixture was stirred at room temperature for 16 h, then evaporated under reduced pressure to give a crude oil. Silica gel column chromatography purification using 5% of methanol in methylene chloride afforded **16** as a white solid (138 mg, 91%). R_f 0.20 (95:5 CH_2Cl_2/MeOH). Mp 88–90 °C. ^{1}H NMR ($CDCl_3+CD_3OD$) δ 2.23 (m, 1H), 2.34 (m, 1H), 3.63 (dd, 1H, $J=11.9$ and 3.9 Hz), 3.77 (dd, 1H, $J=3.3$ and 11.9 Hz), 3.95 (m, 1H), 4.24 (m, 1H), 4.63 (t, 1H, $J=7.0$ Hz), 7.04 (t, 1H, $J=7.3$ Hz), 7.20 (m, 2H), 7.50 (d, 2H, $J=7.6$ Hz), 9.40 (s, 1H, NH). ^{13}C NMR ($CDCl_3+CD_3OD$) δ 39.19, 61.24, 70.75, 77.69, 86.99, 120.34, 124.86, 128.96, 129.16, 130.02, 137.08, 172.34. MS (ES) $m/z=260$ $[M+Na]^+$, 238 $[M+H]^+$. Anal. calcd for $C_{12}H_{15}NO_4$: C, 60.75; H, 6.37; N, 5.90. Found: C, 60.70; H, 6.31; N, 5.85.

***C*-(2′-Deoxy-β-D-ribofuranosyl-1′)-N-[3-(2-acetylamino-thiazole-4-yl)phenyl]carboxamide (17).** By the same procedure as described for the synthesis of **16**, **13** (320 mg, 0.52 mmol) was converted into compound **17** (white solid, 190 mg, 97%). R_f 0.16 (95:5 CH_2Cl_2/MeOH). Mp 180–182 °C. ^{1}H NMR ($CDCl_3$ + DMSO-d_6) δ 2.25 (s, 3H), 2.30 (m, 2H), 3.69 (m, 1H), 3.81 (m, 1H), 3.97 (m, 1H), 4.34 (m, 1H), 4.64 (t, 1H, $J=7.0$ Hz), 5.02 (d, 1H, $J=4.3$ Hz), 5.32 (t, 1H, $J=4.8$ Hz), 7.22 (s, 1H), 7.33 (t, 1H, $J=7.9$ Hz), 7.55 (t, 2H, $J=8.3$ Hz), 8.24 (s, 1H), 9.85 (s, 1H), 10.92 (s, 1H). ^{13}C NMR ($CDCl_3$ + DMSO-d_6) δ 21.88, 38.58, 59.77, 69.06, 77.04, 86.33, 106.66, 116.77, 118.53, 120.60, 128.09, 134.44, 137.68, 148.41, 157.50, 168.09, 171.18. MS (FAB) $m/z=384$ $[M+Li]^+$. Anal. calcd for $C_{17}H_{19}N_3O_5S$: C, 54.10; H, 5.07; N, 11.13. Found: C, 53.81; H, 5.11; N, 10.89.

***C*-(2′-Deoxy-β-D-ribofuranosyl-1′)-*N*-[3-(2-*N*-methyl-*N*-*tert* - butoxycarbonyl - thiazole - 5 - yl)phenyl]carboxamide (18).** By the same procedure as described for the synthesis of **16**, **15** (491 mg, 0.71 mmol) was converted into compound **18** (white solid, 300 mg, 93%). R_f 0.17 (95:5 CH_2Cl_2/MeOH). Mp 190–192 °C. ^{1}H NMR ($CDCl_3$) δ 1.59 (s, 9H), 2.33 (m, 2H), 3.55 (s, 3H), 3.73 (m, 1H), 3.85 (m, 1H), 3.94 (m, 1H), 4.34 (m, 1H), 4.63 (t, 1H, $J=7.2$ Hz), 4.91 (d, 1H, $J=4.6$ Hz), 5.23 (t, 1H, $J=5.1$ Hz), 7.26 (m, 2H), 7.62 (d, 2H, $J=9.7$ Hz), 7.84 (s, 1H), 9.81 (s, 1H). ^{13}C NMR ($CDCl_3$) δ 27.50, 33.22, 39.09, 60.01, 69.27, 77.27, 82.50, 86.56, 116.44, 118.43, 120.76, 121.43, 123.83, 128.72, 131.82, 132.18, 132.60, 160.05, 171.59. MS (ES) $m/z=472$ $[M+Na]^+$, 450 $[M+H]^+$. Anal. calcd for $C_{21}H_{27}N_3O_6S$: C, 56.11; H, 6.05; N, 9.35. Found: C, 56.01; H, 5.79; N, 9.22.

C-(2′-Deoxy-5′-*O*-dimethoxytrityl-β-D-ribofuranosyl-1′)-*N*-phenylcarboxamide (19). Compound **16** (120 mg, 0.5 mmol) was dissolved in dry DMF (8 mL). Triethylamine (3 equiv, 0.2 mL), and DMTCl (1.5 equiv, 250 mg) were successively added. The mixture was stirred at room temperature for 4 h, then quenched by addition of methanol and solvents were evaporated. The crude product was dissolved in ethyl acetate and the organic phase washed with water, dried ($MgSO_4$), and concentrated in vacuo. Silica gel column chromatography purification using 30% of ethyl acetate, 1% of triethylamine in heptane afforded **19** as a white foam (215 mg, 80%). R_f 0.26 (1:1 heptane/ethyl acetate). ^{1}H NMR ($CDCl_3$) δ 2.38 (m, 2H), 3.21 (dd, 1H, $J=4.4$ and 10.3 Hz), 3.42 (dd, 1H, $J=3.9$ and 10.3 Hz), 3.74 (s, 6H), 4.13 (m, 1H), 4.36 (m, 1H), 4.72 (t, 1H, $J=7.8$ Hz), 6.77

(dd, 4H, $J=1.4$ and 8.8 Hz), 7.09 (m, 1H), 7.15–7.41 (m, 16H), 8.60 (s, 1H). ^{13}C NMR ($CDCl_3$) δ 38.93, 54.87, 62.89, 66.05, 72.24, 76.28, 86.06, 86.26, 112.91, 119.65, 124.07, 126.68, 127.63, 127.77, 128.54, 129.65, 135.30, 136.67, 144.01, 158.27, 170.49. MS (ES) $m/z=562$ $[M+Na]^+$, 303 $[DMT]^+$.

***C*-(2′-Deoxy-5′-*O*-dimethoxytrityl-β-D-ribofuranosyl-1′)-*N*-[3-(2-acetylaminothiazole-4-yl)phenyl] carboxamide (20).** By the same procedure as described for the synthesis of **19**, **17** (150 mg, 0.4 mmol) was converted into compound **20** (white foam, 220 mg, 81%). R_f 0.30 (1:4 heptane/ethyl acetate). ^1H NMR ($CDCl_3$) δ 2.20 (s, 3H), 2.45 (m, 2H), 3.23 (dd, 1H, $J=10.5$ and 4.5 Hz), 3.43 (dd, 1H, $J=3.5$ and 10.5 Hz), 3.71 (s, 6H), 4.15 (m, 1H), 4.40 (m, 1H), 4.79 (t, 1H, $J=7.7$ Hz), 6.75 (d, 4H, $J=8.7$ Hz), 6.86 (s, 1H), 7.18–7.49 (m, 13H), 7.90 (s, 1H), 8.77 (s, 1H), 10.10 (s, 1H). ^{13}C NMR ($CDCl_3$) δ 23.18, 39.52, 55.30, 72.55, 78.04, 86.68, 108.18, 113.36, 118.04, 119.56, 122.05, 127.10, 128.06, 128.17, 129.28, 130.07, 135.13, 135.61, 137.47, 144.46, 149.50, 158.25, 158.64, 168.10, 171.48. MS (FAB) $m/z=680$ $[M+H]^+$, 303 $[DMT]^+$.

***C*-(2′-Deoxy-5′-*O*-dimethoxytrityl-β-D-ribofuranosyl-1′)-*N*-[3-(2-*N*-methyl-*N*-*tert*-butoxycarbonyl-thiazole-5-yl)-phenyl]carboxamide (21).** By the same procedure as described for the synthesis of **19**, **18** (220 mg, 0.49 mmol) was converted into compound **21** (white foam, 300 mg, 81%). R_f 0.40 (1:1 heptane/ethyl acetate). ^1H NMR ($CDCl_3$) δ 1.59 (s, 9H), 2.42 (m, 2H), 3.25 (dd, 1H, $J=10.4$ and 4.3 Hz), 3.40 (dd, 1H, $J=10.4$ and 3.5 Hz), 3.54 (s, 3H), 3.68 (s, 6H), 4.14 (m, 1H), 4.41 (dd, 1H, $J=4.1$ and 7.9 Hz), 4.73 (t, 1H, $J=7.8$ Hz), 6.72 (d, 4H, $J=8.6$ Hz), 7.15–7.28 (m, 11H), 7.40 (m, 2H), 7.59 (s, 1H), 8.71 (s, 1H). ^{13}C NMR ($CDCl_3$) δ 27.68, 33.41, 38.81, 54.60, 62.69, 71.82, 77.41, 82.81, 86.05, 112.70, 116.86, 118.59, 121.63, 126.50, 127.42, 127.60, 128.92, 129.42, 132.21, 132.78, 135.02, 135.09, 137.12, 143.76, 158.04, 160.35, 170.69. MS (ES) $m/z=774$ $[M+Na]^+$, 752 $[M+H]^+$, 303 $[DMT]^+$.

Phosphoramidite (22). A solution of compound **19** (150 mg, 0.27 mmol) and *N,N′*-diisopropylethylamine (2 equiv, 100 μL) in 5 mL of anhydrous methylene chloride, under an inert atmosphere, was treated with 2-cyanoethyl diisopropyl-chlorophosphoramidite (70 μL, 1.2 equiv). After stiring for 15 min at room temperature, the reaction mixture was poured into aq $NaHCO_3$ solution, extracted and whashed twice with water. The organic layer was separated, dried over $MgSO_4$, filtred and the solvent removed in vacuo. The crude residue was purified by silica gel chromatography using ethyl acetate/heptane (1/9) as solvants with triethylamine (1%) to provide **22** as a white foam (130 mg, 63%, mixture of two diastereoisomers). R_f 0.57 and 0.62 (1:1 heptane/ethyl acetate). ^{31}P NMR ($CDCl_3$, 243 MHz) δ 147.00, 147.84. MS (ES) $m/z=762$ $[M+Na]^+$, 303 $[DMT]^+$.

Phosphoramidite (23). By the same procedure as described above for the synthesis of phosphoramidite **22**, compound **20** (150 mg, 0.22 mmol) was converted into phosphoramidite **23** (white foam, 140 mg, 73%, mixture of two diastereoisomers). R_f 0.30 and 0.38 (1:1 heptane/ethyl acetate). ^{31}P NMR ($CDCl_3$, 243 MHz) δ 147.08, 147.86. MS (ES) $m/z=903$ $[M+Na]^+$, 881 $[M+H]^+$, 303 $[DMT]^+$.

Phosphoramidite (24). By the same procedure as described above for the synthesis of phosphoramidite **22**, compound **21** (200 mg, 0.26 mmol) was converted into phosphoramidite **24** (white foam, 200 mg, 80%, mixture of two diastereoisomers). R_f 0.56 and 0.60 (1:1 heptane/ethyl acetate). ^{31}P NMR ($CDCl_3$, 243 MHz) δ 147.02, 147.83. MS (ES) $m/z=952$ $[M+H]^+$, 303 $[DMT]^+$.

Automated oligonucleotides synthesis

Oligonucleotides 18-mer were synthesized on a 1-μmol scale using an Biosystem 392 synthesizer employing the standard phosphoramidite chemistry. Following the solid-phase synthesis of oligonucleotides, they were cleaved from the solid support by treatment with concentrated ammonia (30%) for 24 h at room temperature. The 5′-DMT protected oligonucleotides were purified by reversed-phase HPLC (Waters PrepPak Cartridge Delta-Pak C18, 15 μm, 300 Å, 25*100 mm) using a 30 min linear gradient of solvent **A** (0.1 M triethylammonium acetate buffer (pH 7) containing 7% of CH_3CN) and solvent **B** (CH_3CN) (100:0 to 60:40) at a flow rate of 5 mL/min. The DMT and Boc protecting groups were cleaved by treatment with 80% aq AcOH solution for 60 min at room temperature and the mixture was extracted twice with diethylether (20 mL). The oligomers were precipitated using a AcONa buffer (pH 6.2)/EtOH solution and centrifugation at 0 °C for 15 min. The pure oligonucleotides were subjected to analytic HPLC (Waters Delta-Pak C18, 5 μm, 300 Å, 3.9*150 mm), UV (260 nm) analysis and MALDI-TOF mass spectrometry for identification. MALDI-TOF-MS 18TC-$\mathbf{S_{a1}}$: calcd for $C_{178}H_{232}N_{39}O_{119}P_{17}$ $(M-H)^-$: 5348, Found 5348. 18TC-$\mathbf{S_{a1}}$: calcd for $C_{182}H_{236}N_{41}O_{119}P_{17}S$ $(M-H)^-$: 5461, Found: 5461. 18TC-$\mathbf{S_a}$: calcd for $C_{183}H_{236}N_{41}O_{120}P_{17}S$ $(M-H)^-$: 5491, Found: 5489. 18TC-$\mathbf{S_1}$: calcd for $C_{183}H_{238}N_{41}O_{119}P_{17}S$ $(M-H)^-$: 5477, Found: 5475. 18TC-TSC: calcd for $C_{184}H_{238}N_{41}O_{120}P_{17}S$ $(M-H)^-$: 5503, Found: 5500. 18TC-CST: calcd for $C_{183}H_{237}N_{42}O_{119}P_{17}S$ $(M-H)^-$: 5488, Found: 5488. 18TC-CSC calcd for $C_{182}H_{236}N_{43}O_{118}P_{17}S$, $(M-H)^-$: 5473), Found: 5471.

Melting temperature experiments

All thermal denaturation studies were carried out on a Uvikon 940 spectrophotometer and interfaced to an IBM-AT computer for data collection and analysis. Temperature control of the cell holder was achieved by a Haake D8 circulating water bath. The temperature of the water bath was increased from 0 to 90 °C and decreased back to 0 °C at a rate of 0.15 °C/min with absorption readings at 260, 295, 500 nm taken every 1 °C. The maxima of the first derivatives of the melting curves gave a good approximation of the half-dissociation temperature (T_m) and allowed us to characterise the stabilities of the complexes in a reproducible way. The

DNA melting experiments were carried out in a 10-mM cacodylate buffer (pH 6.0) containing 100 mM NaCl, 10 mM $MgCl_2$ and 0.5 mM spermine.

Acknowledgements

The authors thank M. Thomas for oligonucleotide synthesis, Dr. J.-C. Blais for MALDI-TOF/MS characterisation of TFO. We also acknowledge the ANRS for financial support and CNRS for a doctoral fellowship (BDI) to DG. Thanks are also due to Dr. P. Vierling for useful discussions.

References and Notes

1. The symbols • and x indicate Watson–Crick and Hoogsteen hydrogen bonds, respectively.
2. (a) Le Doan, T.; Perrouault, L.; Praseuth, D.; Habhoub, N.; Decout, J. L.; Thuong, N. T.; Lhomme, J.; Hélène, C. *Nucleic Acids Res*. **1987**, *15*, 7749. (b) Moser, H. E.; Dervan, P. B. *Science* **1987**, *238*, 645. (c) For reviews see: Thuong, N. T.; Hélène, C. *Angew. Chem., Int. Ed. Engl*. **1993**, *32*, 666. (d) Frank-Kamenetskii, M. T.; Mirkin, S. M. *Annu. Rev. Biochem*. **1995**, *64*, 65. (e) Neidle, S. *Anti-Cancer Drug Des*. **1997**, *12*, 433.
3. (a) Maher, J. L., III *Cancer Invest*. **1996**, *14*, 66. (b) Giovannangeli, C.; Hélène, C. *Antisense Nucleic Acid Drug Dev*. **1997**, *7*, 413. (c) Vasquez, K. M.; Wilson, J. H. *Trends Biochem. Sci*. **1998**, *23*, 4. (d) Praseuth, D.; Guieysse-Peugeot, A. L.; Hélène, C. *Biochim. Biophys. Acta* **1999**, *1489*, 181.
4. (a) Mergny, J. L.; Sun, J. S.; Rougée, M.; Garestier, T.; Barcelo, F.; Chomilier, J.; Hélène, C. *Biochemistry* **1991**, *30*, 9791. (b) Greenberg, W. A.; Dervan, P. B. *J. Am. Chem. Soc*. **1995**, *117*, 5016. (c) Best, G. C.; Dervan, P. B. *J. Am. Chem. Soc*. **1995**, *117*, 1187.
5. Reviews: (a) Sun, J. S.; Hélène, C. *Cur. Opin. Struct. Biol*. **1993**, *3*, 345. (b) Doronina, S. O.; Behr, J. P. *Chem. Soc. Rev*. **1997**, 63. (c) Gowers, D. M.; Fox, K. R. *Nucleic Acids Res*. **1999**, *27*, 1569, and references cited therein.
6. (a) Griffin, L. C.; Kiessling, L. L.; Beal, P. A.; Gillespie, P.; Dervan, P. B. *J. Am. Chem. Soc*. **1992**, *114*, 7976. (b) Koshlap, K. M.; Gillespie, P.; Dervan, P. B.; Feigon, J. *J. Am. Chem. Soc*. **1993**, *115*, 7908. (c) Huang, C. Y.; Cushman, C. D.; Miller, P. S. *J. Org. Chem*. **1993**, *58*, 5048. (d) Huang, C. Y.; Miller, P. S. *J. Am. Chem. Soc*. **1993**, *15*, 10456. (e) Huang, C. Y.; Bi, G.; Miller, P. S. *Nucleic Acids Res*. **1996**, *24*, 2606. (f) Lehmann, T. E.; Greenberg, W. A.; Liberles, D. A.; Wada, C. K.; Dervan, P. B. *Helv. Chim. Acta* **1997**, *80*, 2002.
7. (a) Durland, R. H.; Rao, T. S.; Bodepudi, V.; Seth, D. M.; Jayaraman, K.; Revankar, G. R. *Nucleic Acids Res*. **1995**, *23*, 647. (b) Zhou, B.; Puga, E.; Sun, J. S.; Garestier, T.; Hélène, C. *J. Am. Chem. Soc*. **1995**, *117*, 10425. (c) Kukreti, S.; Sun, J. S.; Garestier, T.; Hélène, C. *Nucleic Acids Res*. **1997**, *25*, 4264. (d) Kukreti, S.; Sun, J. S.; Loakes, D.; Brown, D. M.; Nguyen, C. H.; Bisagni, E.; Garestier, T.; Hélène, C. *Nucleic Acids Res*. **1998**, *26*, 2179. (e) Gianolio, D. A.; McLaughlin, L. W. *J. Am. Chem. Soc*. **1999**, *121*, 6334.
8. Communications: (a) Guianvarc'h, D.; Benhida, R. *Fourrey, J-L., Maurisse, R. and Sun, J. S., Chem. Commun* **2001**, 1814. (b) Guianvarc'h, D.; Fourrey, J.-L.; Maurisse, R.; Sun, J. S.; Benhida, R. *Org. Lett*. **2002**, *4*, 4209.
9. (a) Basha, A.; Lipton, M.; Weinreb, S. M. *Tetrahedron Lett*. **1977**, *48*, 4171. (b) Lipton, M. F.; Basha, A.; Weinreb, M. *Org. Synth*. **1979**, *59*, 49.
10. Hovinen, J.; Salo, H. *J. Chem. Soc., Perkin Trans. 1* **1997**, 3017.
11. Benhida, R.; Lecubin, F.; Fourrey, J.-L.; Quintero, L. *Tetrahedron Lett*. **1999**, *40*, 5701.
12. (a) Stille, J. K. *J. Am. Chem. Soc*. **1979**, 4992. (b) Stille, J. K. *Angew. Chem., Int. Ed. Engl*. **1986**, *25*, 508.
13. Compound **5** was obtained in three steps from 2-aminothiazole (see ref 8b).
14. Hoffer, M. *Chem. Ber*. **1960**, *93*, 2777.
15. We observed that the procedure using diethylaluminium cyanide (Iyer, R.P.; Phillips, L.R.; Egan, W. *Synth. Commun*. **1991**, *21*, 2053) or sodium or potassium cyanide (Kolb, A.; Huynh Dinh, T.; Igolen, J. *Bull. Soc. Chim. France* **1973**, 3447) gave low diastereoselectivity and low chemical yields because the deprotection of toluoyl protecting groups was principally observed. The introduction of nitrile group was done using TMSCN and $BF_3{\cdot}Et_2O$ leading to a 1:3 mixture of α/β anomers in 90% yield.
16. Mukayiama, T.; Usui, M.; Shimada, E.; Saigo, K. *Chem. Lett*. **1975**, 1045.
17. The DNA melting experiments were carried out in a 10 mM cacodylate buffer (pH 6.0) containing 0.1 M NaCl, 10 mM $MgCl_2$ and 0.5 mM spermine.
18. Kiessling, L. L.; Griffin, L. C.; Dervan, P. B. *Biochemistry* **1992**, *31*, 2829.
19. (a) NMR structural studies of the A•Tx**G** triplet have explained this stabilization by the existence of a favourable stacking interaction between guanine (of the triplet A•Tx**G**) and the thymine on the 5′-side (Radhakrishnan, I.; Gao, X.; De Los Santos, C.; Live, D.; Patel, D. J. *Biochemistry* **1991**, *30*, 9022). (b) Such a favourable stacking can also explain the lower stability obtained in presence of C^+ at positions Z_1 and/or Z_2 when Z = **S**.
20. In a similar work on compound $\mathbf{D_3}$, a 4-(5-benzimidazophenyl)imidazole nucleobase that was found to equally stabilise the triplex at both A•T and G•C sites, Dervan et al. have shown that in a triplex containing an A•Tx$\mathbf{D_3}$ triplet, only the 3′-neighbouring triplet affected the triplex stability.[18] Later, NMR experiments showed $\mathbf{D_3}$ to be intercalated between the A•T inverted base pair and the 3′ neighbouring triplet thus explaining the 3′ neighbour effect (Koshlap, K.M.; Gillespie, P.; Dervan, P.B.; Feigon, J. *J. Am. Chem. Soc*. **1993**, *115*, 7908). In the case of **S**, this absence of 3′ or 5′ effect seems to be in favour of a recognition process which involves hydrogen bond contacts.